

Derivation of persistent time for anisotropic migration of cells*

Yan-Ping Liu(刘艳平)¹, Xiao-Cui Zhang(张晓翠)¹, Yu-Ling Wu(吴宇宁)¹, Wen Liu(刘雯)¹,
Xiang Li(李翔)^{1,2}, Ru-Chuan Liu(刘如川)³, Li-Yu Liu(刘雳宇)³, and Jian-Wei Shuai(帅建伟)^{1,2,4,†}

¹Department of Physics, Xiamen University, Xiamen 361005, China

²State Key Laboratory of Cellular Stress Biology, Innovation Center for Cell Signaling Network, Xiamen University, Xiamen 361102, China

³College of Physics, Chongqing University, Chongqing 401331, China

⁴Research Institute for Biomimetics and Soft Matter, Fujian Provincial Key Laboratory for Soft Functional Materials Research, Xiamen University, Xiamen 361102, China

(Received 5 September 2017; revised manuscript received 15 September 2017; published online 20 November 2017)

Cell migration plays an essential role in a wide variety of physiological and pathological processes. In this paper we numerically discuss the properties of an anisotropic persistent random walk (APRW) model, in which two different and independent persistent times are assumed for cell migrations in the x - and y -axis directions. An intrinsic orthogonal coordinates with the primary and non-primary directions can be defined for each migration trajectory based on the singular vector decomposition method. Our simulation results show that the decay time of single exponential distribution of velocity auto-correlation function (VACF) in the primary direction is actually the large persistent time of the APRW model, and the small decay time of double exponential VACF in the non-primary direction equals the small persistent time of the APRW model. Thus, we propose that the two persistent times of anisotropic migration of cells can be properly estimated by discussing the VACFs of trajectory projected to the primary and non-primary directions.

Keywords: cell migration, random walk, Langevin equation, cancer

PACS: 87.17.Aa, 05.40.Fb, 87.19.xj, 05.10.Gg

DOI: 10.1088/1674-1056/26/12/128707

1. Introduction

Cell migration plays an essential role in a wide variety of physiological and pathological processes, including embryogenesis, nervous development, wounding healing, inflammation, metastasis and immune reactions.^[1] Regulated by complex cellular signaling pathways, cell migration is critical and indispensable for the normal development of organs and tissues.^[2–4] The onset of migration in a mature organism is often associated with some human diseases, such as cancer.^[5]

As an important biological behavior, cell motility has also attracted much attention of biophysics for a long time.^[6] The migration of cells can be simply treated as a persistent random walk (PRW). The phenomenon of random walk has been studied in statistical physics since the beginning of last century. The PRW of cells can be phenomenologically described by the Ornstein–Uhlenbeck (OU) process with the following Langevin equation for velocity vector v :^[7]

$$\frac{dv}{dt} = -\frac{1}{\tau}v + \frac{\sqrt{2D}}{\tau}\xi(t), \quad (1)$$

where t is the time, τ is the persistent time, D is the diffusion coefficient characteristic derived from Brownian motion, and $\xi(t)$ represents the random vector of a Wiener process.

With only two parameters, i.e., diffusion coefficient D and persistence time τ in Eq. (1), the PRW model is one of the simplest and popular models for cell motility. To reflect the intensity of the current cell memory of past velocity, the PRW model describes cell trajectory as a succession of correlated movements within a duration equal to the persistence time τ . An isotropic environment is also assumed for cell migration in PRW model. As a result, the PRW describes a normal diffusive process, and so the mean squared displacement grows linearly with time on a long time scale. The PRW model also gives a simple Gaussian distribution of velocities, a single-exponential decay of the auto-correlation function (ACF) of velocity, an isotropic velocity field and a flat distribution of angles between cell movements on a long time scale.

In addition to the simple PRW model, there are various cell types modulated by different migration signaling pathways in different complex cellular environments.^[1] Thus, researchers have found experimentally that many cells exhibit more complex migration properties which conflict with the prediction of simple PRW model. Unlike the normal diffusion, the anomalous diffusion movement has been observed in some cell types. Regulated by chemokine CXCL10, CD8+ T-cell behavior is similar to a generalized Lévy walk in order to find rare targets in an optimal strategy.^[8] An exponential

*Project supported by the National Natural Science Foundation of China (Grant Nos. 31370830, 11675134, 11474345, and 11604030), the State Key Development Program for Basic Research of China (Grant No. 2013CB837200), the 111 Project, China (Grant No. B16029), and the China Postdoctoral Science Foundation (Grant No. 2016M602071).

†Corresponding author. E-mail: jianweishuai@xmu.edu.cn

distribution of velocity has been found in the study of long-term cell migration in low-density monolayer cultures,^[9] and the Tsallis' distribution of velocity has been observed for endodermal hydra cells in cellular aggregates.^[10] The motility of human keratinocytes and fibroblasts cell types presents a double-exponential decay for the velocity ACF (VACF).^[11] Recent experiments reveal that the complex three-dimensional (3D) environments can cause more interesting behaviors of cell migration.^[12] The metastatic breast cancer cells invade a 3D collagen matrix in a cooperative manner by exchanging leaders in the invading front.^[13,14] It has been shown that the migration of fibrosarcoma cells in 3D extracellular collagen matrices is anisotropic, generating an anisotropic velocity field.^[15,16]

As a result, different models have been proposed to explain different migration behaviors of cells.^[17,18] Some models in fact are the modified PRW models,^[11,15,16,19] but more models are quite different from PRW model.^[9,14,17,18,20–23] Among these models, by incorporating anisotropic space into the PRW model, an anisotropic PRW (APRW) model has been recently proposed to describe the migration of cells in 3D collagen matrix.^[15] Compared with other migration models, the APRW model is still simple enough, because it just considers two different persistent times and two different diffusion coefficients in migration directions of x axis and y axis. The APRW model predicts a double-exponential ACF of velocity, anisotropic velocity profile and anisotropic distribution of angular displacement, which can adequately explain the behaviors of 3D cell motility over a wide range of matrix densities.^[15,16]

Although the APRW model has been proposed to simulate the cell migration in 3D collagen matrix, the full characterization of VACF has not yet been presented for APRW model. Importantly, it remains unclear if one can, based on the trajectories of mobile cells, quantitatively derive the two persistence times of random walk, which can reflect the anisotropy of cell migration. In the paper, we numerically discuss APRW model in detail. Our simulation results show that one can obtain the two persistent times by discussing the VACFs of trajectory velocity.

2. APRW model

In APRW model, the migration cells have different persistent times (P_x, P_y) and mobile speeds (S_x, S_y) in the directions of x -axis and y -axis, respectively.^[15] So, the propagation of cell location is given by

$$\begin{aligned} x(t + dt) &= x(t) + dx(t, dt), \\ y(t + dt) &= y(t) + dy(t, dt). \end{aligned} \quad (2)$$

Here, dx and dy are the displacements of cell location in the x - and y -axis directions in time steps of dt . The displacements

of cell location over time are governed by the following equations:

$$\begin{aligned} dx(t, dt) &= \alpha_x \cdot dx(t - dt, dt) + F_x \cdot W, \\ dy(t, dt) &= \alpha_y \cdot dy(t - dt, dt) + F_y \cdot W, \end{aligned} \quad (3)$$

where $W \sim N(0, 1)$ is the white noise. To incorporate the anisotropic migration of cells, the parameters of the persistent times (P_x, P_y) and the cell speeds (S_x, S_y) along the x - and y - axis directions are different from each other, leading to the following equations:^[15]

$$\begin{aligned} \alpha_x &= 1 - \frac{dt}{P_x}, \quad \alpha_y = 1 - \frac{dt}{P_y}, \\ F_x &= \sqrt{\frac{S_x^2 dt^3}{P_x}}, \quad F_y = \sqrt{\frac{S_y^2 dt^3}{P_y}}. \end{aligned} \quad (4)$$

In the model, if we set $P_x = P_y$ and $S_x = S_y$, the APRW model becomes the classic PRW model.

3. Simulation results

It has been shown that there should be a relationship between the cell persistent time and mobile speed.^[24,25] However, for simplicity we assume $S_x = S_y = 0.6 \mu\text{m}/\text{min}$ in all the simulations in the model. The time step $dt = 0.01 \text{ min}$ is used in our programming simulation. With the recording time interval $\Delta t = 1 \text{ min}$, each trajectory is recorded with a length of 10^4 min for cell migration. Considering the effects of noises on migratory trajectories,^[19] 1000 trajectories are typically averaged at the level of population to obtain statistical results.

3.1. Trajectory and velocity

For comparison, we first plot 1000 trajectories for PRW model with $P_x = P_y = 2 \text{ min}$ and for APRW model with $P_x = 10 \text{ min}$ and $P_y = 2 \text{ min}$ in Figs. 1(a) and 1(b), respectively. In the figure, all the 1000 trajectories are plotted, with the starting points located at the origin (0, 0). The distribution of trajectories obtained with PRW model looks like similar in all directions, because it is an isotropic model. However, the APRW model generates the migration trajectories exhibiting an anisotropic distribution. With a larger memory time of $P_x = 10 \text{ min}$, the migration movements of cells typically have less stochasticity along the x -axis, and so the trajectories distribute in a wider range along the x axis than the y axis.

With the trajectory $\mathbf{r}(t)$, the velocity vector $\mathbf{v}(t)$ can be obtained with $\mathbf{v}(t) = (\mathbf{r}(t) - \mathbf{r}(t - \Delta t)) / \Delta t$. As an example, the values of speed $v(t) = \sqrt{v_x^2 + v_y^2}$ of a single trajectory of cell migration generated by PRW model and APRW model are plotted in Figs. 1(c) and 1(d), respectively. The averaged velocities over 1000 trajectories with two models are also shown in Figs. 1(c) and 1(d). Both cells display the motile behaviors with a similar mean speed because of the same S used in two models.

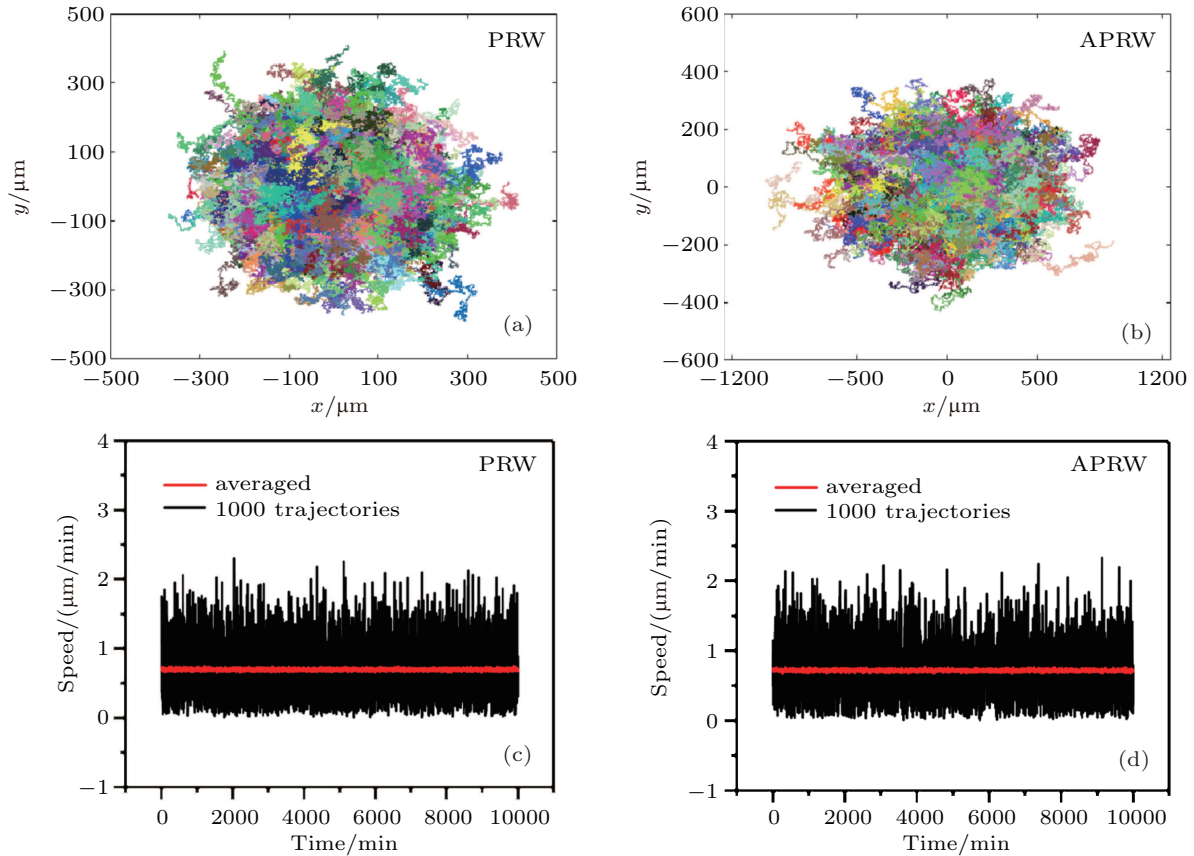


Fig. 1. (color online) The 1000 migration trajectories generated by (a) PRW model with $P_x = P_y = 2$ min and (b) APRW model with $P_x = 10$ min and $P_y = 2$ min. All 1000 trajectories are plotted with different colors, with the starting points located at the origin (0, 0). The velocity of a single trajectory of cell migration and the averaged velocity over 1000 trajectories generated by (c) PRW model with $P_x = P_y = 2$ min and (d) APRW model with $P_x = 10$ min and $P_y = 2$ min.

3.2. VACF in x and y components

Now we discuss the VACF of APRW model, which is defined by the following equation^[21]

$$\begin{aligned}
 & c(t_{\text{lag}}) \\
 &= \frac{N-1}{N-l-1} \\
 & \times \frac{\sum_{j=1}^{N-l} \left(\mathbf{v}_j - \frac{1}{N-l} \sum_{i=1}^{N-l} \mathbf{v}_i \right) \cdot \left(\mathbf{v}_{j+l} - \frac{1}{N-l} \sum_{i=l+1}^N \mathbf{v}_i \right)}{\sum_{j=1}^N \left(\mathbf{v}_j - \frac{1}{N} \sum_{i=1}^N \mathbf{v}_i \right)^2} \quad (6)
 \end{aligned}$$

with $t_{\text{lag}} = l\Delta t$. In Eq. (6), the terms subtracted in the numerator and denominator are considered in order to remove bias which results from the finite trajectory length. However, this process causes another small bias, which can be removed by considering factor $(N-1)/(N-l-1)$ in Eq. (6).^[21] The final VACF is an average of $c(t_{\text{lag}})$ over 1000 trajectories.

In Eq. (6), the VACF is written in the form of velocity vector, which has to be split into x and y components for calculation in detail. As a result, we have $c(t_{\text{lag}}) = c_x(t_{\text{lag}}) + c_y(t_{\text{lag}})$ with VACFs of $c_x(t_{\text{lag}})$ and $c_y(t_{\text{lag}})$ in x and y components, respectively. In fact, the cell migrations along x and y axes are independent of each other in the APRW model. Thus, the

two-dimensional (2D) APRW migration can be treated as a linear superposition of the two independent one-dimensional (1D) PRW migrations along x and y axes, resulting in the VACF of 2D APRW, a double exponential decay described by $e^{-t/P_x} + e^{-t/P_y}$.^[15]

In Fig. 2(a), the VACFs are calculated with $P_y = 2$ min and P_x varying from 2 min to 30 min. For the PRW model with $P_x = P_y = 2$ min, the VACF presents single exponential decay as $e^{-t/\tau}$ with $\tau = 2$ min. While for the APRW model with large P_x , the VACF clearly shows a double exponential distribution of $e^{-t/\tau_x} + e^{-t/\tau_y}$. Projecting velocity vectors into x and y directions, the corresponding VACFs in x and y components exhibit the behavior of single exponential decay. The fitted decay times τ_x and τ_y are plotted in Fig. 3(b) each as a function of P_x , giving $\tau_x = P_x$ and $\tau_y = P_y = 2$ min as expected.

This discussion indicates that the two persistent times of APRW model can be simply obtained by discussing the VACFs in x and y components, respectively. But such a calculation requires a prior knowledge of the directions of P_x and P_y , which have been set to be along the x and y axes in our simulation. However, the directions of P_x and P_y of migration trajectories of cells in biological experiment are actually unknown, causing such a scheme practically useless.

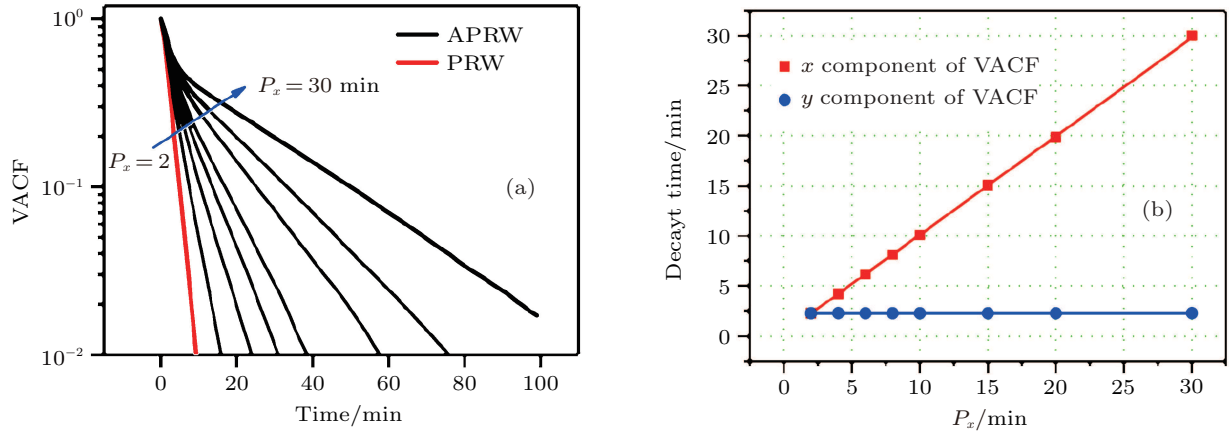


Fig. 2. (color online) VACFs of APRW model with (a) $P_y = 2$ min and $P_x = 4, 6, 8, 10, 15, 20,$ and 30 min and (b) two decay times fitted with double exponential distribution against P_x . The results for PRW model with $P_x = P_y = 2$ min are also given in the figure.

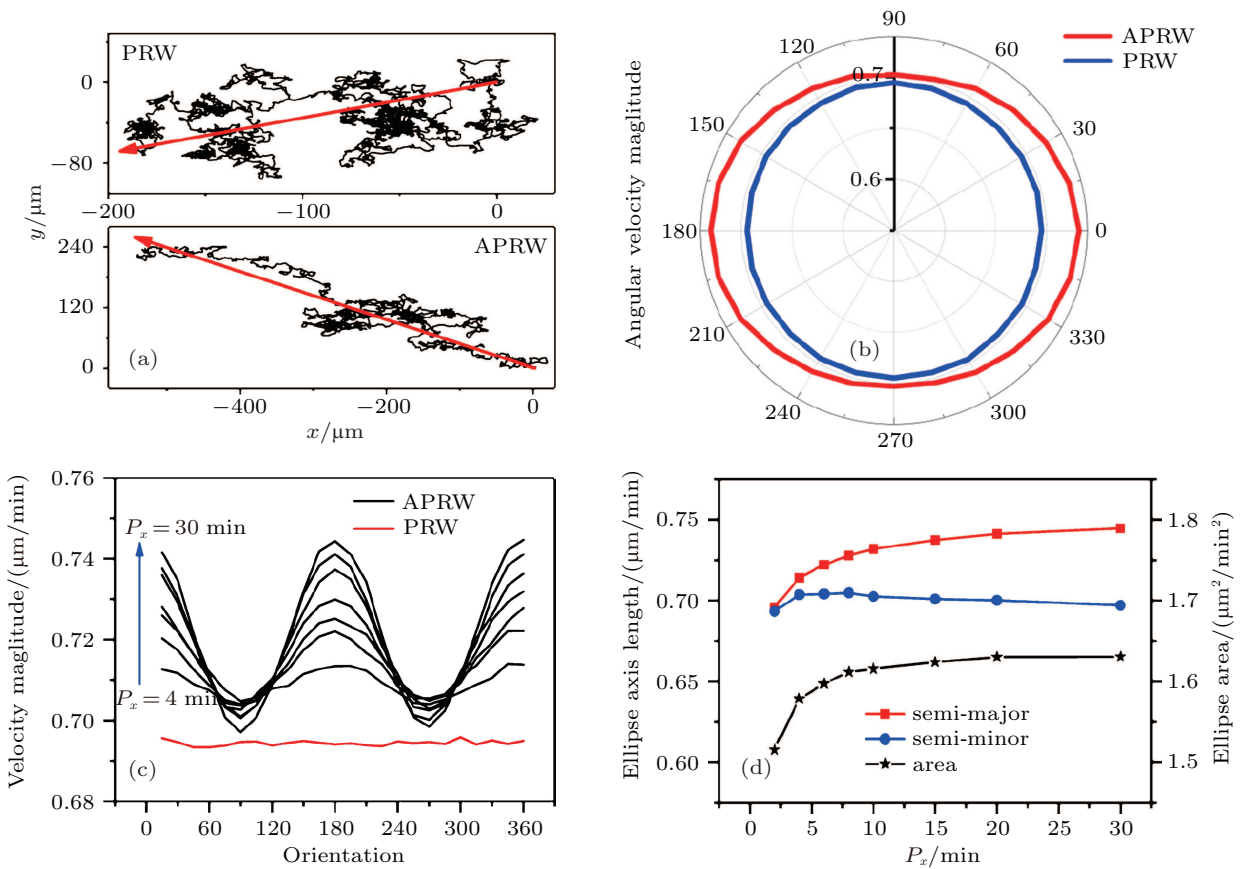


Fig. 3. (color online) (a) trajectories generated by PRW model (upper panel) and APRW model (lower panel), and the corresponding primary directions \mathbf{p} . (b) Polar plots of the velocity magnitude at different orientation angles with respect to the primary direction \mathbf{p} of cell trajectories. The blue circle is for PRW model at $P_x = P_y = 2$ min and the red ellipse is for APRW model at $P_x = 10$ min and $P_y = 2$ min. (c) Velocity magnitudes versus orientation angle. (d) Semi-major and semi-minor axes, as well as the area of the ellipse, against the persistent time P_x .

3.3. Primary direction and angular velocity magnitude

It has been suggested that the primary direction (\mathbf{p}) and non-primary direction ($n\mathbf{p}$) obtained with the singular vector decomposition (SVD) can be defined as the intrinsic axes of the migration trajectory.^[15] With the SVD, the velocity matrix M of individual cells can be expressed as

$$M = U\Sigma V^* \quad (7)$$

where U is the matrix eigenvectors of the product MM^* , V is the matrix eigenvectors of the product M^*M , Σ are the singular values of the matrix M , and $*$ denotes the transposed matrix. The first and second eigenvector of V^* correspond to primary and non-primary directions of individual trajectory, respectively. Thus, one can define an intrinsic orthogonal coordinates for each trajectory.

As examples, the trajectories generated by the PRW and

APRW models, as well as the corresponding primary directions \mathbf{p} , are shown in Fig. 3(a). The primary direction \mathbf{p} of these two trajectories is different from the direction of x axis. Then the orientation angle between velocity direction and primary direction at each time step can be calculated. As a result, the velocity magnitudes at different orientation angles with respect to the primary direction \mathbf{p} can be statistically obtained over 1000 cell migrations. Figure 3(b) shows the polar plots of the averaged velocity magnitude at different orientation angles with PRW model at $P_x = P_y = 2$ min and APRW model at $P_x = 10$ min and $P_y = 2$ min. A circular velocity magnitude has been obtained with the PRW model. Differently, an ellipse of velocity magnitude is found in the polar plot with the APRW model, indicating a longer persistent time along the primary direction.

For a better illustration of the effect of local anisotropy on velocity magnitude, the relationship between velocity magnitude and orientation angle is drawn in the orthogonal coordinates in Fig. 3(c). The PRW model generates an almost horizontal line with a velocity magnitude around 0.725 for orientation angle ranging from 0° to 360° , giving an isotropic movement in all directions. While the APRW model gives waving curves, all of which look like a letter “W”. In detail, the velocity magnitude reaches minimal values at orientation angles of 90° and 270° corresponding to non-primary direction, while reaches maximal values at orientation angles of 0° (360°) and

180° corresponding to primary direction. With the increase of the persistent time P_x , the waving amplitude becomes larger, indicating an increasing anisotropy.

For an ellipse distribution of the velocity magnitude in polar coordinate, the semi-major and semi-minor axes of ellipse can be obtained from the primary and non-primary directions, respectively. In Fig. 3(d), both the semi-major and semi-minor axes are plotted each as a function of P_x . With the increase of P_x , the semi-major axis increases slightly, while the semi-minor axis increases first and then decreases slightly. The area of the ellipse, which is the product of π and the two lengths, are also shown in Fig. 3(d). At a small value of P_x , the ellipse area increases with increasing P_x . Then the ellipse area approaches to a constant value at large P_x .

3.4. VACF in \mathbf{p} and $n\mathbf{p}$ components

With the primary and non-primary components serving as the intrinsic orthogonal coordinates for individual trajectories, all the velocity vectors with time can be projected to \mathbf{p} and $n\mathbf{p}$ directions. Then the VACFs at \mathbf{p} and $n\mathbf{p}$ directions can be calculated for each trajectory. Figure 4 shows the plots of the averaged VACFs at \mathbf{p} and $n\mathbf{p}$ directions over 1000 trajectory versus time for the APRW model. The VACF in the \mathbf{p} direction typically exhibits a single exponential decay, while the VACF in the $n\mathbf{p}$ direction shows a distribution of double exponential decay.

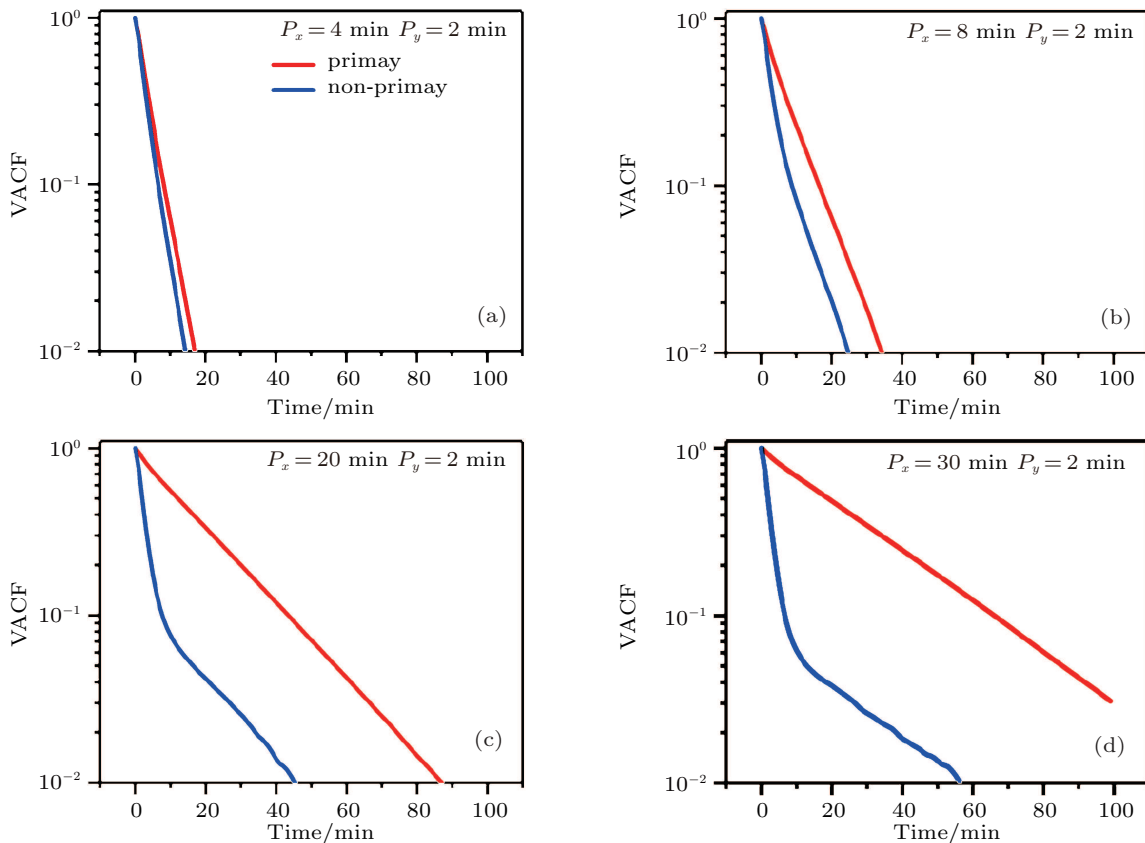


Fig. 4. (color online) VACFs in primary direction \mathbf{p} and non-primary direction $n\mathbf{p}$ of APRW model with $P_y = 2$ min and $P_x = 4$ (a), 8 (b), 20 (c), and 30 min (d). Red line represents VACFs in \mathbf{p} direction and the blue lines in $n\mathbf{p}$ direction.

Thus, we use $e^{-t/\tau}$ to fit the VACF in the p direction, and $e^{-t/\tau_1} + e^{-t/\tau_2}$ to fit the VACF in the np direction by using software Origin2017. The obtained decay time τ in the p direction versus P_x is plotted in Fig. 5(a). An interesting observation is that the exponential fitting gives a relationship of $\tau = P_x$. Thus, even by discussing the VACF along primary direction, the obtained exponential decay time can satisfactorily reveal the value of large persistent time of the APRW model. Figure 5(b) shows the plot of the decay times τ_1 and τ_2 in the np direction against P_x . Here, the small decay time almost keeps constant at 2 min with varying P_x . As a result, the result of $\tau_1 = P_y = 2$ min indicates that the small decay time obtained from VACF along the non-primary direction can properly reflect the value of small persistent time of APRW model.

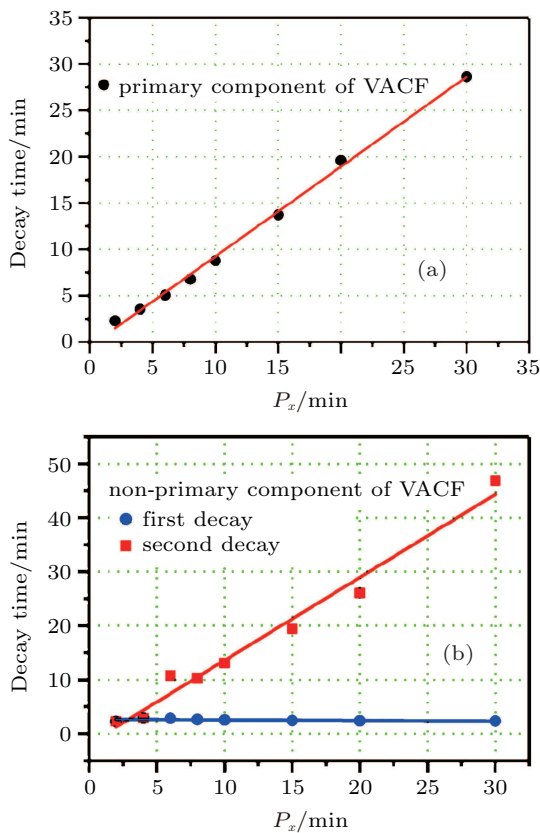


Fig. 5. (color online) Plots of exponential decay time τ in (a) p direction and decay times τ_1 and τ_2 in (b) np direction versus P_x .

4. Conclusions

In order to describe the cell migration in 3D collagen matrix, an anisotropic persistent random walk model is suggested.^[15,16] Compared with the classic PRW model, the APRW model contains some different assumptions in order to consider two different and independent persistent times and mobile speeds for cell migration in the x and y axes, respectively. Because the dynamical behaviors of APRW model have not yet been systematically investigated, we carry out the numerical simulation to discuss the various properties of APRW model in detail.

An important question with APRW model is whether the basic parameters of two persistence times along the x and y axes can be properly calculated only by discussing the migration trajectories. We show that if a prior knowledge of the directions of P_x and P_y is given, one can directly project the migration velocities of cells into such orthogonal coordinates. Then the VACFs on the two axes of such orthogonal coordinates will simply exhibit a distribution of single exponential decay, with the decay times exactly equal to P_x and P_y . However, such a scheme is practically useless, because one could not have a prior knowledge of the directions of P_x and P_y in biological experiment.

The only information one has in experiment is the trajectories of migration cells. For each trajectory, one can define the primary and non-primary directions by velocity matrix based on the singular vector decomposition method. As a result, the intrinsic orthogonal coordinates of the primary and non-primary directions can be obtained for each trajectory. The anisotropic migration behaviors, including ellipse distribution of velocity magnitude at polar plot, can be discussed according to the intrinsic orthogonal coordinates.

By projecting the migration velocity to the intrinsic orthogonal coordinate, the VACF at primary direction typically exhibits a single exponential decay, while the VACF at non-primary direction shows a distribution of double exponential decay. Importantly, our simulation results show that the decay time of single exponential VACF in the primary direction equals the large persistent time of the APRW model, and the small decay time of double exponential VACF in the non-primary direction equals the small persistent time of the APRW model.

In experiment, the double exponential VACFs are observed with anisotropic migrations for various cell types. Our work indicates that the two persistent times of the biological trajectory of cell migration can be properly estimated by discussing the VACFs of trajectory velocities projected to the intrinsic orthogonal coordinates of the primary and non-primary directions. The information of two persistent times will quantitatively reveal how anisotropic the cell migration is, which may be caused by anisotropic environment.

In our model, the cell migrates only with different persistent times of P_x and P_y along the x and y axis, but with the same mobile speeds along the x and y axes, i.e., $S_x = S_y$. It has been suggested that there should be a relationship between the cell persistent time and diffusion coefficient,^[24,25] because the anisotropic environment typically causes not only the different persistent times, but also the different diffusion coefficients in different directions. Thus, how to derive correctly all the persistent times and the diffusion coefficients in different directions from the migration trajectories remains an interesting problem to be discussed in the future research.

References

- [1] Douglas A Lauffenburger and Alan F Horwitz 1996 *Cell* **84** 359
- [2] Anne J Ridley, Martin A Schwartz, Keith Burridge, Richard A Firtel, Mark H Ginsberg, Gary Borisy, Thomas Parsons J and Alan Rick Horwitz 2003 *Science* **302** 1704
- [3] Mccann C, Kriebel P, Parent C A and Losert W 2010 *J. Cell Sci.* **123** 1724
- [4] Dang I, Gorelik R, Sousablin C, *et al.* 2013 *Nature* **503** 7475
- [5] Peter Friedl and Darren Gilmour 2009 *Nat. Rev. Mol. Cell Biology* **10** 445
- [6] Berg H C 1983 *Physics Today* **40** 73
- [7] Uhlenbeck G E and Ornstein L S 1930 *Phys. Rev.* **36** 823
- [8] Tajie H Harris, Edward J Banigan, David A Christian, *et al.* 2012 *Nature* **486** 545
- [9] András Cziráok, Katalin Schlett, Emília Madarász and Tamás Vicsek 1998 *Phys. Rev. Lett.* **81** 3038
- [10] Upadhyaya A, Rieu J P, Glazier J A and Sawada Y 2001 *Physica A* **293** 549
- [11] Selmeczi D, Mosler S, Hagedorn P H, Larsen N B and Flyvbjerg H 2005 *Biophys. J.* **89** 912
- [12] Driscoll M K and Danuser G 2015 *Trends in Cell Biology* **25** 749
- [13] Liyu Liu, Guillaume Duclos, Bo Sun, *et al.* 2013 *Proc. Natl. Acad. Sci. USA* **110** 1686
- [14] Jiangrui Zhu, Long Liang, Yang Jiao and Liyu Liu 2015 *PLOS One* **10** e0118058
- [15] Wu P, Giri A, Sun S X and Wirtz D 2014 *Proc. Natl. Acad. Sci. USA* **111** 3949
- [16] Wu P, Giri A and Wirtz D 2015 *Nature Protocols* **10** 517
- [17] Metzler R and Klafter J 2000 *Phys. Rep.* **339** 1–77
- [18] Mandelbrot B B and Van Ness J W 2006 *Siam Review* **10** 422
- [19] Stokes C L, Lauffenburger D A and Williams S K 1991 *J. Cell Sci.* **99** 419
- [20] Campos D, Mendez V and Llopis I 2010 *J. Theor. Biology* **267** 526
- [21] Li L, Cox E C and Flyvbjerg H 2011 *Physical Biology* **8** 046006
- [22] Höfling F and Franosch T 2013 *Rep. Prog. Phys.* **76** 046602
- [23] Zaburdaev V, Denisov S and Klafter J 2015 *Rev. Mod. Phys.* **87** 483
- [24] Maiuri P, Rupprecht J, Wieser S, *et al.* 2015 *Cell* **161** 374
- [25] Baumann K 2015 *Nat. Rev. Mol. Cell Biology* **16** 267